A versatile biomimetic controller for contact tooling and haptic exploration

Gowrishankar Ganesh, Nathanael Jarrasse, Sami Haddadin, Alin
Albu-Schaeffer, Etienne Burdet

HAL Id: hal-02110723
https://hal.science/hal-02110723

Submitted on 25 Apr 2019

A versatile biomimetic controller for contact tooling and haptic exploration

Gowrishankar Ganesh*, Nathanael Jarrassé* , Sami Haddadin, Alin Albu-Schaeffer and Etienne Burdet

Abstract— This article presents a versatile controller that enables various contact tooling tasks with minimal prior knowledge of the tooled surface. The controller is derived from results of neuroscience studies that investigated the neural mechanisms utilized by humans to control and learn complex interactions with the environment. We demonstrate here the versatility of this controller in simulations of cutting, drilling and surface exploration tasks, which would normally require different control paradigms. We also present results on the exploration of an unknown surface with a 7-DOF manipulator, where the robot builds a 3D surface map of the surface profile and texture while applying constant force during motion. Our controller provides a unified control framework encompassing behaviors expected from the different specialized control paradigms like position control, force control and impedance control.

I. Introduction

While recent studies have shown that tool usage is not restricted to human activities [1], [2], the exceptional ability of man to use a wide array of tools still distinguishes him from other animals. It would thus be a major achievement if similar abilities could be obtained in robots. Based on investigation [3] and modelling of how humans interact with their environment [4], [5], this paper develops and tests a controller that enables robots to control different tooling tasks by adapting the impedance, force and trajectory plan of the robot as humans do.

Though current industrial robots already use tools, they work in well-controlled environments and are mostly involved in non-contact tooling tasks such as welding and gas cutting, where the robot does not physically come in contact with the tooled object. Surface exploration is probably the only application where current robot manipulators make purposeful contact with the external objects. Surface exploration is performed either by pure haptics [6]–[10] or aided by vision [11], [12] but utilizes minimal contact forces. It aims to either form a 3D model of the object [13]–[15] or determine the texture of the object [16], for which dedicated sensors and controls have been proposed [17], [18]. The control of the robot during non-contact tool tasks and surface exploration is thus relatively easy because of the specialized sensors and due to the fact that the controller has to deal only with the robot kinematics and dynamics, which are (assumed to be) known.

In contrast, the challenge in controlling contact tool tasks like polishing, carving, cutting, drilling or writing, is to follow a given surface profile (similar to surface exploration tasks) while maintaining a significant force on the surface. A contact-tool task is influenced by the dynamics of the robot, and also by that of the tooled surface, which is normally unknown. Furthermore, the presence of a large contact force makes the task highly unstable to disturbances caused by friction, irregularities in the surface or noise in the robot motor output. The robot requires to maintain the right impedance to counter these instabilities. Contact tooling usually involves penetration of the external surface of an object. Therefore vision and surface exploration do not help in determining the irregularities and variations within the external surface.

When the tool task and environment are well known, specific controllers can be implemented to perform the task. For example, a drilling task may be achieved with stiff position control or modifications of impedance control [19] (though the task instability will require careful tuning of impedance), and exploration of simple surfaces may be achieved using hybrid control [19], [20] by controlling position tangential to the surface and force normal to it. However, *the challenge is to develop a versatile controller able to handle all these tasks with minimal prior knowledge about the tooled surface*.

Compared to current robots, humans are very versatile and interact with all kinds of objects apparently without requiring specialized controllers. Based on the model of human motor adaptation we have recently discovered [4], [5], this paper introduces a versatile controller for the interaction of a robot with the environment. The bio-mimetic algorithm, which is an extension of [21], [22], enables robots to perform (unstable) contact tooling on unknown surfaces similar to humans. We simulate the performance of the algorithm in three typical contact tasks: surface exploration, drilling and cutting. Finally, we show results of a pilot surface exploration experiment utilizing a 7-DOF robot manipulator to explore a test surface.

II. Human-like motor adaptation

Humans excel in the ability to adapt rapidly to the variable dynamics of their arm as the hand interacts with the environment. Mussa-Ivaldi and his collaborators have studied this adaptation by letting subjects perform planar arm reaching movements while interacting with a velocity dependent force field [23]. They could show that the human central nervous system adapts feedforward control during repeated trials by compensating for the environment forces,

which can be modelled by nonlinear adaptive control [24], [25].

However, this does not explain how humans can learn unstable tasks common in daily life [26], e.g. many tasks involving tools such as using a screwdriver or drilling, where interaction and motor noise are amplified by the applied force. In the last ten years, we have addressed learning of unstable tasks in humans in a series of experimental studies [3], [27]–[29]. We could show that humans are also able to adapt impedance independently from force by selective activation of suitable muscles groups.

Humans adapt both force and impedance to perform stable and unstable tasks skilfully [26]. This can be modelled by a control law with feedforward and feedback:

$$w = u + v, \quad (1)$$

where the variables are functions of time. In this equation, w is the motor command, which is composed of a feedforward term u and a feedback term v, that typically results from muscle intrinsic properties and neural feedback, i.e. reflexes. The simple principles of motor learning based on our experimental results [4] yield that humans adapt feedforward and feedback during movement by concurrent minimization of instability, error and effort in motor command.

Our previous work [21] exhibited how a bio-mimetic algorithm based on these principles (and expressed in joint space) can give human like dexterity to robots while ensuring stability [22]. The algorithm used in this article is a derivative of that proposed in [21] implemented in task space.

The robot control torque is given by Equ.(1) with

$$v = Ke + D\dot{e}, \quad e = x_r - x, \quad (2)$$

where x represents the task space coordinates of the end effector and error signal e is calculated with respect to the reference trajectory $x_r(t)$. K and D are diagonal positive matrices (so with positive components in the diagonal and other components 0). The feedforward force and mechanical impedance are adapted as:

$$\Delta u^k \equiv u^{k+1} - u^k \equiv \alpha v^k - (1-\mu)u^k, \ 0 < \alpha, \mu < 1 \quad (3)$$
$$\Delta K_{ii}^k \equiv K_{ii}^{k+1} - K_{ii}^k \equiv \beta \mid v_i^k \mid -\gamma, \quad \beta, \gamma > 0 \quad (4)$$

where k is the trial or time index and α, β, γ and μ represent learning parameters. The damping D is set as

$$D_{ii}^k \equiv 2\sqrt{K_{ii}^k} \quad (5)$$

corresponding to critical damping.

In Equ.(4) stiffness increases with the rectified feedback, such that the control gains K and D increase with any error, contributing to reducing error, and superfluous stiffness is eliminated by the decay γ. Feedforward force adaptation, which is similar to iterative learning, compensates for reproducible forces in the task dynamics through reducing feedback forces [30], which in turn helps keeping stiffness at a low value. In fact, stiffness increases only in the presence of random perturbations which cannot be learnt by feedforward adaptation and just after novel dynamics are introduced. The

convergence properties of this learning controller have been examined in [22].

The forgetting factor of μ in the feedforward learning is necessary to relax force when no negative feedback is available for this purpose, for example during a surface exploration task (explained later) where the reference always stays inside the explored surface.

The reference trajectory is adapted (slightly differently from the previous work [21]) as:

$$\Delta x_r^k \equiv x_r^{k+1} - x_r^k \equiv \delta(x_f - x_r^k), \quad 0 < \delta < 1. \quad (6)$$

The term

$$x_f \equiv x^k - \frac{n\rho}{K_{min}}, \quad (7)$$

where ρ represents the desired contact force, K_{min} is the specified minimum of K and n is the unit vector normal to the surface, which can be detected by internal sensing at the robot's endpoint, or extrapolated from the surface's part previously explored. The reference adaptation thus aims at moving the reference towards and near the actual position of the end effector but inside the object with which the robot interacts, such that constant contact force is equal to the specified value would be applied when stiffness is minimum.

III. TOOL TASK SIMULATIONS

We simulated three typical contact tooling tasks to exhibit the abilities of the controller. In all these tasks the default learning parameters were $\alpha \equiv 0.05$, $\mu \equiv 0$, $\beta \equiv 7$, $\gamma \equiv 0.005$, $\delta \equiv 0.01$. Particular learning parameters which were set to zero in each task are mentioned during each task description.

A. Tool and Surface model

The tool was modelled as a point mass in two degrees-of-freedom (with x_1 in the forward direction and x_2 normal to the surface as is shown in Fig.1) which was controlled by the algorithm. This corresponds to using the algorithm in the task space of a robot manipulator. In all the simulations, the tool was assumed to be of significantly higher stiffness and hardness than the material being tooled, such that there is no deformation of the tool during interaction.
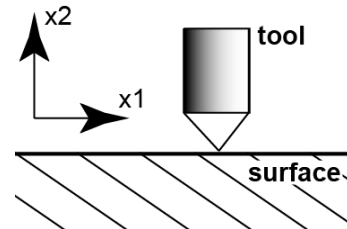

Fig. 1.   Coordinate system definition

The model of the surface was defined in such a way that:
- for the drilling and cutting tasks, an unknown threshold force is required for the tool to penetrate the surface and once it is inside a large damping force is applied opposed to the normal (penetration) x_2 direction.

- In addition, for the drilling task, the tool encounters sinusoidal *horizontal* force perturbations (along x_1). This simulates the vibrations generated by the drilling process.
- For the cutting task, when the tool reached the desired cutting depth, a high frequency, low amplitude sinusoidal *vertical* (along x_2) force simulates the perturbing force noise generated by a material and its internal texture. Also along the forward direction, some dry friction (proportional to the force applied normally by the tool) requires the forward force to reach a certain level for the tool to start moving. In this case, a large damping force has been added to resist the forward *horizontal* movement once the tool is inside the surface.
- For the surface exploration task, a surface was used which is composed of a rising and then falling ramp, an area similar to a "macro velcro" (geometrically modelled as a high frequency low amplitude sinusoidal position perturbations) and finally a large sinusoidal profile. Some dry friction (proportional to the normal force applied on the surface) was added once again along the forward *horizontal* direction, along with some damping resistive force when the tool is in contact with the surface. In this specific scenario the tool also experiences an additional spring force (with fixed small gains) towards a (straight line) reference trajectory placed below the surface. This force leads to the appearance of some force perturbations according to the changes in the shape of the impenetrable surface.

B. Task simulations

1) Cutting: In this task the robot is required to make a cut of $d = 3cm$ depth on a surface. This is equivalent to a milling or carving operation and requires:

- a constant feedforward force to cut against the material,
- minimal contact force (normal to direction of cut) to avoid excessive penetration of the surface,
- adjustment of stiffness so as to maintain stability against the irregularities in tooled material.

This operation is difficult to perform with a force-based controller because thorough knowledge of the object would be required to know which force level is required for the cut, complicated by the irregularities. On the other hand, the task may be achieved with position or an impedance controller [19], but the gains of the controller had to be specifically tuned to the surface of interest. This is because during cutting, while some amount of tool stiffness is required to counter the friction, excessive stiffness can get the tool stuck in the material, such as while sawing wood. In contrast, our controller can adjust the stiffness automatically as required by each surface.

Figure 2 shows the normal force, position and stiffness of the robot during the cutting task simulated with our controller. At the beginning of the task, the reference (red trace in Fig.2.B) is set at the required depth below the surface corresponding to the depth of cut required. The reference adaptation Equ.(6) is switched off for this operation. The
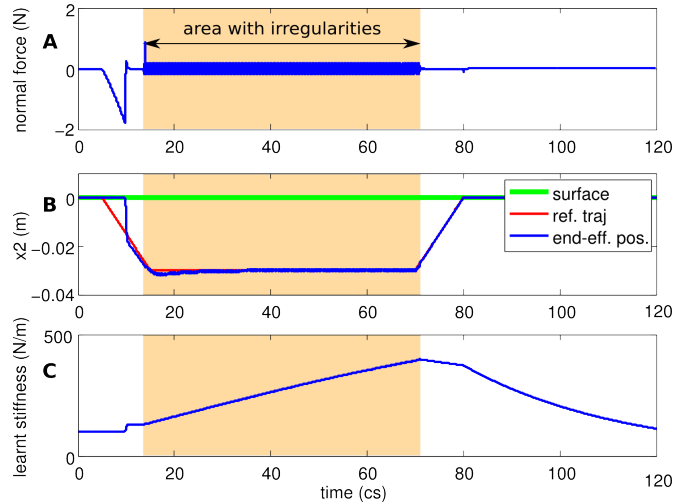

Fig. 2. Cutting task simulation: Task robot variables along x2 direction: (A) contact force, (B) task reference (red) and position of tool(blue), (C) stiffness of the tool along x2. Irregularities in the surface were simulated (orange region) by a sinusoidal external force.

robot first automatically increases the contact force (Fig.2.A) and penetrates to the required depth, then proceeding with a horizontal cut during which the contact force (normal to the cut) is reduced to zero. In the presence of irregularities (marked in Fig.2.A) the robot automatically increases its stiffness (Fig.2.C) with little increase in contact force (note the small perturbations in the orange region in Fig.2B). In the absence of irregularities, and after the end of the cutting operation, the robot automatically reduces its stiffness.

2) Drilling: While drilling is similar to cutting, it usually involves a larger contact force on the surface. This task is inherently unstable, as the heavy drill (and the robot) supported at the end of a narrow tool tip will amplify any noise. A drilling task thus requires:

- constant force and minimal stiffness in the drilling direction,
- stability against the large, random perturbations perpendicular to the drilling direction.

While a force controller can be used to maintain the drilling force, it would require additional control to maintain stability in the lateral direction. Hybrid position-force control [31] or hybrid impedance control [32] are thus probably suited for this operation. However, the controller would still require some additional control along the force controlled (drilling) direction, so as to monitor the movement and increase the controlling force in the presence of obstacles (for instance, a knot in wood would temporarily require more force in the drilling direction).

Our controller provides all these requirements automatically. The trajectory learning Equ.(6) is again switched off in this operation. The feedforward learning in the algorithm (Fig.3.E) adapts the movement force as required and reduces the feedback and hence the feedback gain (Equ.4), making the drill compliant along x2 (Fig.3.F). At the same time, along x1, the algorithm automatically increases stiffness

(Fig.3.C) to stabilize control against perturbations and keep the lateral perturbations low (Fig.3.A). In the presence of some surface obstacles like a knot in the wood (orange region in Fig. 3), the feedback automatically increases force feedforward in the x2 direction (Fig.3.E) temporarily, before bringing it back to the prescribed value. The force dies down when the drilling stops.
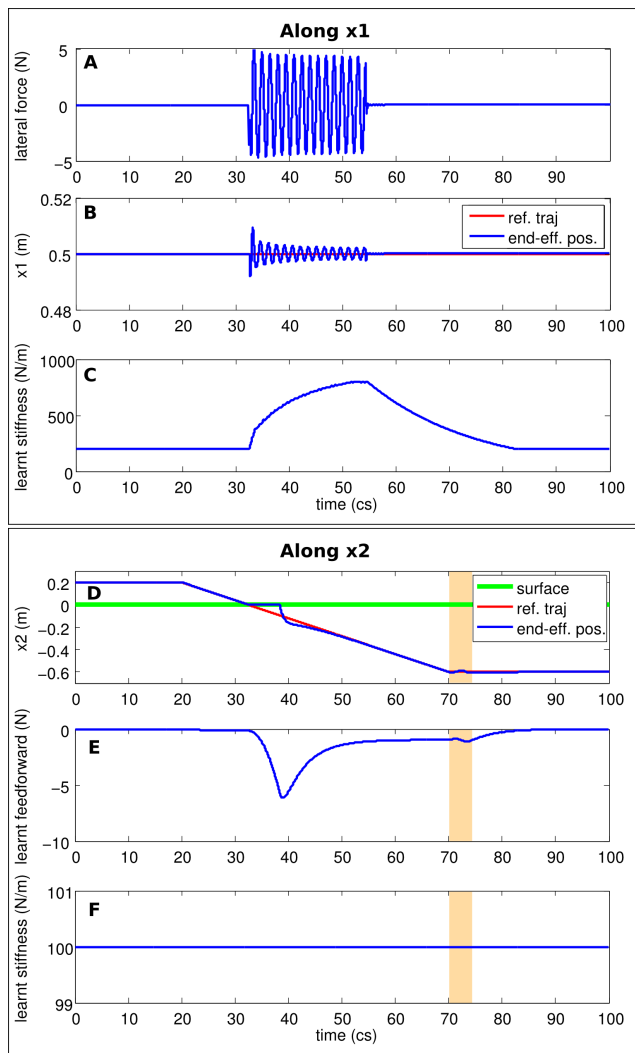

Fig. 3. Drilling task simulation. Along x1: In the presence of perturbations (A) along the x1 direction, lateral to the drilling direction, the robot increases stiffness only along this direction (C) to keep the tool vibrations low (blue trace in B) and close to the reference (red trace in B). Once the vibrations decrease, stiffness is reduced to a low value again. Along x2: position (D), feedforward force (E) and tool stiffness (F). Note that a low stiffness is maintained while feedforward force is learnt to achieve the task. In the presence of an internal obstacle (like a wood knot, during the orange period), the feedforward is automatically increased to counter this, before returning to a lower value.

3) Surface exploration/Polishing: These tasks require:
- robot to glide along unknown surfaces;
- the contact force to be minimum or constant;
- if possible, the robot should be able to acquire some information about the object's "texture".

This operation requires force control normal to the unknown surface and position control tangential to it.

Therefore, some form of a hybrid force-position or force-impedance control seems to be suitable. However, the controller would require a surface estimation algorithm in order to modulate the control dimensions dependent on the object surface as it explores it. Due to the ability to adapt the reference trajectory (Equ.6), our algorithm inherently possesses surface exploration capabilities. Furthermore, we show that stiffness learning during this task estimates the surface texture.
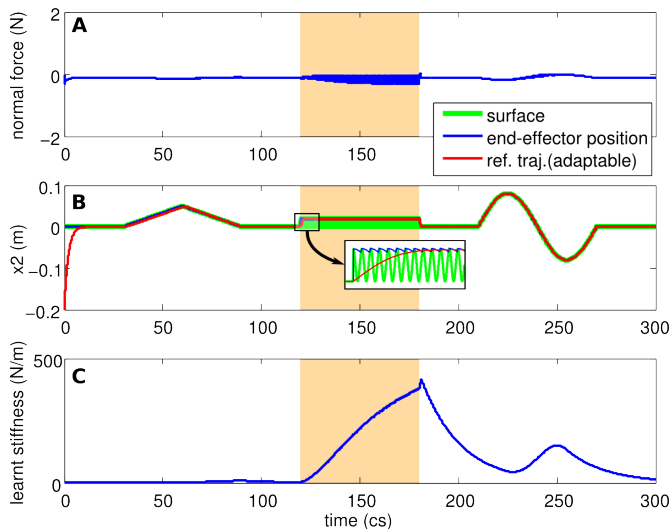

Fig. 4. Surface exploration task simulation: In this task the robot explored an unknown surface and built its map (red trace in B) while moving (blue trace in B). The contact force (along x2) during the movement was maintained (A) at a minimal value while stiffness along x2 increased (C) only in the presence of a rough texture (orange region) on the surface. The stiffness changes could be thus used to identify the texture of the explored surface.

To implement the exploration task with our algorithm, a rough reference trajectory is initially set below the unknown surface (see start of simulation in Fig.4B, where the red trace starts below green) similar to a cutting task. However the difference with respect to the cutting task is that the feedforward force along the normal of the surface is either switched off or limited to a small value in order to avoid cutting of the surface. This allows for the proxy reference trajectory x_r in Equ.(6) to conform to the unknown surface. A simple PD task feedback was added instead of using $\mu > 0$, otherwise with no negative feedback feedforward is increased and the robot raises of the surface. The adapted reference follows the surface (Fig.4B) and in turn may be used to estimate the surface normal and tangent at any time instance. Note that the normal force (Fig.4A) is kept at a low value throughout the movement while the stiffness (Fig.4C) increases only when there are surface irregularities.

IV. EXPERIMENTS

A pilot surface exploration experiment with the DLR light-weight 7-DOF robot manipulator was conducted to test the performance of the algorithm and demonstrate its capabilities. The setup, shown in Fig.5B, required the robot to traverse various surface profiles on a test surface while

maintaining a constant and significant contact force, similar to the polishing of an unknown surface.
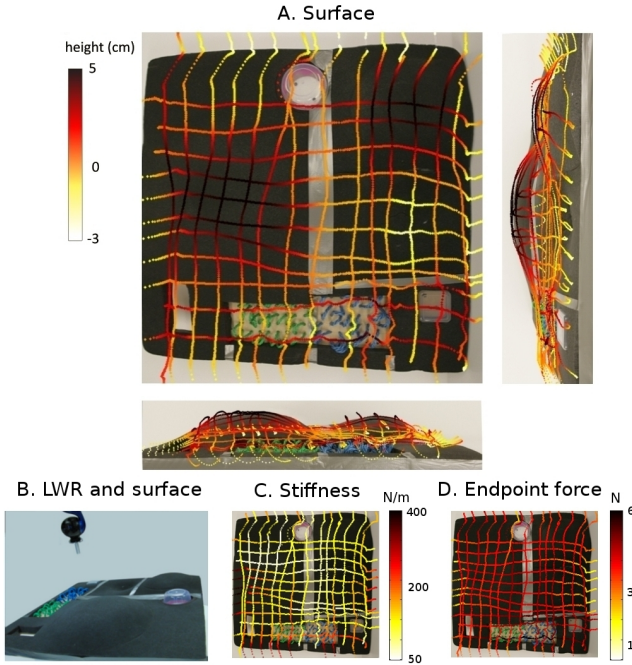

Fig. 5. The testing experiment involved the DLR 7 DOF lightweight arm (LWR) and the test surface shown in (B). The surface identified by the robot by exploration is plotted along the explored trajectory mesh in (A) with the actual surface in the background. (C) and (D) plot the endpoint stiffness and contact force (estimated from the torque sensors on the robot joints) during the exploration. The contact force is roughly maintained at the very low prescribed value of 0.05N while stiffness varies with the surface texture.

A test surface was developed on a wooden plank of size 85x95cm as shown in Fig.5. Various profiles, including convex bumps, concave troughs and cylindrical obstacles were created on this surface by fixing metallic and plastic objects. A 3cm thick layer of packing foam was then overlaid on the surface. The test surface also included a high friction pad created using twisted nylon ropes and a hole in the surface.

The test surface was placed on a table under the 7-DOF manipulandum (as shown in Fig.5.B) which was equipped with a 12cm long aluminium finger at the end-effector (i.e., the seventh joint). The robot reference was set for repetitive to and from movements in the plane of the table over a range of 120cm and with a constant speed of 10cm/s (except for the acceleration and de-accelerations near the workspace boundaries). The reference was set in the task space and the trajectory was developed using the interpolator of the manipulator. The required contact force was set to 0.05N. The test surface was placed in the middle of this range and moved manually such that the robot could "scan" the entire surface.

The learning parameters in the algorithm were set to $\alpha \equiv 0.4$, $\mu \equiv 0.95$, $\beta \equiv 75$, $\gamma \equiv 0.3$, $\delta \equiv 1.2$. The proposed adaptation algorithm runs on top of a low-level controller with 1 kHz rate [33]–[35] and directly commands the desired feedforward torque and impedance to it. The setup is con-
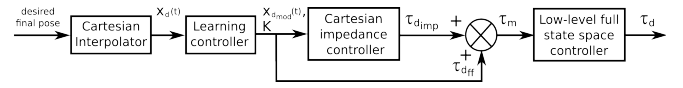

Fig. 6. Concrete implementation of the controller. Such implementation is possible with the Fast Research Interface (FRI) of KUKA® for the LWR robot.

trolled by a QNX real-time PC for low-level control that is connected to a Windows XP PC controlling the non real-time task. A view of the concrete implementation of the controller is shown in Fig.6.

Fig.5A shows the surface traced by the robot. The plot shows the tool-tip coordinates of the robot in the xy plane (plane of the table) with the color gradient representing the z-coordinate (height above the table). Fig.5C plots the endpoint stiffness of the robot as it performed the surface exploration while Fig.5D shows the contact force along the vertical z-axis as estimated from the torque sensors at the robot joints. Note that stiffness is maintained at a similar low value throughout the exploration and increases only in the edges of the surface and in the region with irregularities. The stiffness increase may thus be used to estimate the texture properties of the surface. The contact force is maintained around the specified value of 0.05N.

V. DISCUSSION

This paper introduced a versatile bio-mimetic controller which is able to handle different tooling tasks like humans do. The underlining feature of the controller enabling this is its ability to automatically and simultaneously adjust impedance, feedforward force and trajectory as per the requirement of the environment, through direct mechanical interaction.

Maintaining contact stability is probably the biggest challenge while using tools. Most end-effector held tools require applying a large contact force and are subject to large disturbances due to the irregularities on the tooled surface and hence are inherently unstable. Humans have been shown to be able to modulate their hand impedance skilfully [3] as required by a task to maintain stability. With this algorithm we give similar properties to the robot and ensure maintenance of stability of the robot [22], [36] in these tasks. Feedforward adaptation is essential for tasks like cutting, where the material irregularities continuously change the required cutting force. Feedforward adaptation helps counter these variations while maintaining minimum stiffness of the cutting tool. Trajectory adaptation enables maintenance of contact force during tasks like polishing and prevents the robot from applying very high forces in the presence of unforeseen obstacles.

As in any concrete task, our algorithm does require some basic parameter definition for each tooling operation such as cutting speed and depth of cut prescribed by tool manufacturer for a given tool-surface combination. However, it does not require the definition of any acute details about possible irregularities, surface texture and even shape of the tooled surface. The simulations demonstrated that the same

algorithm can handle different operations without changing its structure, though different applications did require specialization through setting of a parameter to zero. For example, trajectory learning was switched off during the drilling and cutting operation while feedforward learning was switched off during surface exploration. However, note that these definitions are not material or environment specific, but operation specification. In this respect, we provide here a general framework, which encompasses the properties and behavior of many of the previous controllers, including position control, force control, impedance control and hybrid version of these controls.

REFERENCES

[1] FB De Waal. Cultural primatology comes of age. *Nature*, 399(6737):635–636, 1999.

[2] AAS Weir, J Chappell, and A Kacelnik. Shaping of Hooks in New Caledonian Crows. *Science*, 297(5583):981, 2002.

[3] E Burdet, R Osu, DW Franklin, TE Milner, and M Kawato. The central nervous system stabilizes unstable dynamics by learning optimal impedance. *Nature*, 414(6862):446–9, 2001.

[4] DW Franklin, E Burdet, KP Tee, R Osu, CM Chew, TE Milner, and M Kawato. Cns learns stable, accurate, and efficient movements using a simple algorithm. *Journal of Neuroscience*, 28(44):11165–73, 2008.

[5] KP Tee, DW Franklin, M Kawato, TE Milner, and E Burdet. Concurrent adaptation of force and impedance in the redundant muscle system. *Biological Cybernetics*, 102(1):31–44, 2010.

[6] AM Okamura and MR Cutkosky. Haptic exploration of fine surface features. In *Proceedings of the IEEE International Conference on Robotics and Automation*, pages 2930–2936, 1999.

[7] SA Stansfield. Haptic Perception with an Articulated, Sensate Robot Hand. *Robotica*, 10(06):497, 1992.

[8] K Pribadi, JS Bay, and H Hemami. Exploration and dynamic shape estimation by a robotic probe. *IEEE Transactions on Systems, Man and Cybernetics*, 19(4):840–846, 1989.

[9] S Sestili and A Starita. Learning objects by tactile perception. In *Proceedings of the Annual International Engineering in Medicine and Biology Society*, pages 896–897, 1989.

[10] P Dario, M Bergamasco, and A Sabatini. Sensing body structures by an advanced robot system. *Proceedings of the IEEE International Conference on Robotics and Automation*, pages 1758–1763, 1988.

[11] Okamura AM and MR Curkosky. Feature-guided exploration with a robotic finger. *Proceedings of the IEEE International Conference on Robotics and Automation*, pages 589–596, 2001.

[12] HT Tanaka, K Kushihama, N Ueda, and S Hirai. A vision-based haptic exploration. In *Proceedings of the IEEE International Conference on Robotics and Automation*, pages 3441–3448, 2003.

[13] A Bierbaum, M Rambow, T Asfour, and R Dillmann. A potential field approach to dexterous tactile exploration of unknown objects. In *Proceedings of the IEEE-RAS International Conference on Humanoid Robots*, pages 360–366, 2008.

[14] F Mazzini, D Kettler, S Dubowsky, and J Guerrero. Tactile robotic mapping of unknown surfaces: an application to oil well exploration. pages 80–85, 2009.

[15] DR. Faria, R Martins, J Lobo, and J Dias. Probabilistic representation of 3D object shape by in-hand exploration. In *Proceedings of the IEEE/RSJ International Conference on Intelligent Robots and Systems*, pages 1560–1565, 2010.

[16] WW Mayol-Cuevas, J Juarez-Guerrero, and S Munoz-Gutierrez. A first approach to tactile texture recognition. In *Proceedings of the IEEE International Conference on Systems, Man, and Cybernetics*, number 1993, pages 4246–4250, 1998.

[17] D Kraft, A Bierbaum, M Kjaergaard, J Ratkevicius, A Kjaer-Nielsen, C Ryberg, H Petersen, T Asfour, R Dillmann, and N Kruger. Tactile object exploration using cursor navigation sensors. In *Proceedings of the World Haptics- Third Joint EuroHaptics conference and Symposium on Haptic Interfaces for Virtual Environment and Teleoperator Systems*, pages 296–301, 2009.

[18] PA Schmidt, E Mael, RP Wurtz, E Mael, and Rolf P. Wurtz. A sensor for dynamic tactile information with applications in human-robot interaction and object exploration. *Robotics and Autonomous Systems*, 54(12):1005–1014, 2006.

[19] N Hogan. Impedance control: An approach to manipulation. In *Proceedings of the American Control Conference*, pages 304–313, 1985.

[20] O Khatib. A unified approach for motion and force control of robot manipulators: The operational space formulation. *IEEE Journal of Robotics and Automation*, 3(1):43–53, 1987.

[21] G Ganesh, A Albu-Schaeffer, and M Haruno. Biomimetic motor behavior for simultaneous adaptation of force, impedance and trajectory in interaction tasks. *Proceedings of the IEEE International Conference on Robotics and Automation*, pages 2705–2711, 2010.

[22] C Yang, G Ganesh, S Haddadin, S Parusel, A Albu-Schaeffer, and E Burdet. Human-like Adaptation of Force and Impedance in Stable and Unstable Interactions. *IEEE Transaction on Robotics*, 27(5):1–12, 2011.

[23] R Shadmehr and FA Mussa-Ivaldi. Adaptive representation of dynamics during learning of a motor task. *Journal of Neuroscience*, 14:3208–3224, 1994.

[24] M Kawato, K Furukawa, and R Suzuki. A hierarchical neural-network model for control and learning of voluntary movement. *Biological Cybernetics*, 57:169–185, 1987.

[25] Etienne Burdet. *Algorithms of human motor control and their implementation in robotics, PhD Thesis*. PhD thesis, ETH-Zurich, Switzerland, 1996.

[26] E Burdet, KP Tee, I Mareels, TE Milner, CM Chew, DW Franklin, R Osu, and M Kawato. Stability and motor adaptation in human arm movements. *Biological cybernetics*, 94(1):20–32, 2006.

[27] DW Franklin, E Burdet, R Osu, M Kawato, and TE Milner. Functional significance of stiffness in adaptation of multijoint arm movements to stable and unstable dynamics. *Experimental Brain Research*, 151(2):145–157, 2003.

[28] DW Franklin, R Osu, E Burdet, M Kawato, and TE Milner. Adaptation to stable and unstable dynamics achieved by combined impedance control and inverse dynamics model. *Journal of Neurophysiology*, 90(5):3270–3282, 2003.

[29] DW Franklin, G Liaw, TE Milner, R Osu, E Burdet, and M Kawato. Endpoint stiffness of the arm is directionally tuned to instability in the environment. *Journal of Neuroscience*, 27(29):7705–7716, 2007.

[30] E Burdet, A Codourey, and L Rey. Experimental evaluation of nonlinear adaptive controllers. *IEEE Control System Magazine*, 18:39–47, 1998.

[31] MH Raibert and JJ Craig. Hybrid Position/Force Control of Manipulators. *Journal of Dynamic Systems, Measurement, and Control*, 103(2):126–133, 1981.

[32] RJ Anderson and MW Spong. Hybrid impedance control of robotic manipulators. *IEEE Journal of Robotics and Automation*, 4(5):549–556, 1988.

[33] O Eiberger, S Haddadin, M Weis, A Albu-Schaffer, and G Hirzinger. On joint design with intrinsic variable compliance: derivation of the dlr qa-joint. In *Proceedings of the IEEE International Conference on Robotics and Automation*, pages 1687–1694. IEEE, 2010.

[34] LL Tien, A Albu-Schaffer, A De Luca, and G Hirzinger. Friction observer and compensation for control of robots with joint torque measurement. In *Proceedings of the IEEE/RSJ International Conference on Intelligent Robots and Systems*, pages 3789–3795, 2008.

[35] A Albu-Schaffer, C Ott, and G Hirzinger. A unified passivity-based control framework for position, torque and impedance control of flexible joint robots. *International Journal of Robotic Research*, 26(1):23–39, 2007.

[36] E Burdet, G Ganesh, and A Albu-Schaffer. Interaction Force, Impedance and Trajectory Adaptation : by Humans, for Robots. In *Proceedings of the International Symposium on Experimental Robotics*, 2010.